

Red Phosphorescent Iridium(III) Complexes Containing 5-Benzoyl-2-phenylpyridine Derived Ligands with Electron-Donating/-Withdrawing Moieties for Organic Light-Emitting Diodes

KUM HEE LEE,¹ HYUN JU KANG,¹ SEUL ONG KIM,¹
SUK JAE LEE,² JI HYUN SEO,² YOUNG KWAN KIM,²
AND SEUNG SOO YOON¹

¹Department of Chemistry, Sungkyunkwan University, Suwon,
Gyeonggi-do, Korea

²Department of Information Display, Hongik University, Seoul, Korea

A series of red-phosphorescent Ir(III) complexes based on 5-benzoyl-2-phenylpyridine derivatives were synthesized. To explore their electroluminescent properties, multi-layered OLEDs were fabricated the device structure of ITO/2-TNATA/NPB/Ir(III) complexes (8%) doped in CBP/BCP/Alq₃/Liq/Al. The device 2 displays the excellent EL performances; its LE, PE, and EQE reach 30.4 cd/A, 10.1 lm/W, and 8.23% at 20 mA/cm², respectively. The maximum electroluminescence spectrum peak was 571 nm, with the CIE coordinates of (0.486, 0.512) at 12.0 V, and the device also showed a stable color chromaticity with various voltages.

Keywords 5-Benzoyl-2-phenylpyridine ligand; electroluminescence; iridium complex; red phosphorescence

Introduction

Iridium(III) organometallic complexes are explored for a multitude of interest in a variety of photonic applications. Especially, the charged compounds have been intensely studied for use as dopants in light-emitting electrochemical cells (LEECs) [1,2] and the neutral ones in organic/organometallic light-emitting diodes (OLEDs) [1–3]. In contrast with the fluorescent emission, the electrophosphorescence is easily harnessed from both singlet and triplet excited states. Thus, their internal quantum efficiency can reach a theoretical level of unity rather than the 25% inherent upper limit imposed by the formation of singlet excitons for the respective fluorescent materials [4]. Fortunately, this upper limit can be overcome by using phosphorescent complexes as a dopant in OLEDs to harvest both singlet and triplet excitons. This

Address correspondence to Prof. Seung Soo Yoon, Department of Chemistry, Sungkyunkwan University, Cheoncheon-dong, Jangan-gu, Suwon, Gyeonggi-do, 440-746 Korea (ROK). Tel.: (+82)31-290-7071; Fax: (+82)31-290-5971; E-mail: ssyoon@skku.edu

phenomenon increases the internal quantum efficiency to that of almost 100% [5–7]. The highly efficient phosphorescence emission is attributed to the strong spin-orbit coupling of the electronic state by the heavy-atom effect of the metal, which can facilitate the singlet-triplet spin crossover [8,9].

In this paper, a series of red phosphorescent Ir(III) complexes based on benzoylated phenylpyridine ligands were synthesized and their electrophosphorescent properties were investigated. The electron-donating group (-OMe) and electron-withdrawing group (-CF₃) were introduced to tune the band gap of iridium complexes by the control HOMO or LUMO energy levels [10–14]. Multilayered organic light-emitting diodes (OLEDs) were fabricated to explore their electroluminescent properties by employing the complexes as dopant and revealed that these new Ir(III) complexes (1–3) had highly efficient electroluminescent properties.

Experimental

General Procedure for the Synthesis of Ir(III) Complexes

L1 [15] (0.68 g, 2.2 mmol) was dissolved in 2-ethoxyethanol (9 mL) in a 30 mL round-bottom flask. IrCl₃ · 3H₂O (0.30 g, 1.0 mmol) and water (3 mL) were then added to the flask. The mixture was stirred under nitrogen at 120°C for 24 h and cooled to room temperature. The precipitate formed in the mixture was collected and washed with methanol, hexane and dried in vacuum to give the corresponding cyclometalated Ir(III)-μ-chloro-bridge dimer. In a 20 mL flask, the dimer complex, acetylacetone (1.5 mL, 1.5 mmol) and Na₂CO₃ (0.32 g, 3.0 mmol) were mixed with 2-ethoxyethanol (10 mL) and mixture was heated at 100°C for 6 h. After cooling to room temperature, the precipitation solid was collected by filtration, washed with ethanol and hexane. The residue was dissolved in dichloromethane, and then the solid was filtered off. The solution was concentrated in vacuo and the residue was purified on a silica gel column using dichloromethane and hexane as eluent. The product was obtained after recrystallization from dichloromethane/ethanol. Similar procedures were also employed for the synthesis of other iridium complexes. The yields and spectral data of all iridium complexes are as follows.

Compound 1 (Bzppy)₂Ir(acac). The yield of 39%. ¹H-NMR (300 MHz, CDCl₃): δ 8.89 (d, *J* = 1.2 Hz, 2H), 8.30 (dd, *J* = 1.8 Hz, 8.4 Hz, 2H), 7.98 (d, *J* = 8.7 Hz, 2H), 7.83–7.80 (m, 4H), 7.65–7.58 (m, 4H), 7.53–7.48 (m, 4H), 6.86 (td, *J* = 1.2 Hz, 7.5 Hz, 2H), 6.74 (td, *J* = 1.5 Hz, 7.5 Hz, 2H), 6.30 (dd, *J* = 1.2 Hz, 7.8 Hz, 2H), 5.29 (s, 1H), 1.55 (s, 6H); ¹³C-NMR (125 MHz, CDCl₃): δ 192.9, 185.2, 172.5, 151.0, 150.6, 143.6, 138.8, 137.2, 133.7, 133.0, 130.8, 130.6, 130.1, 128.9, 125.9, 121.5, 118.4, 100.9, 28.8; IR (KBr): 3054, 2999, 1659, 1597, 1577, 1515, 1434, 1399, 1315, 1284, 1265, 947, 739, 712, 661 cm⁻¹; FAB-MS (*m/z*): 808 [M⁺]. HRMS-FAB⁺ calcd for C₄₁H₃₁IrN₂O₄ 808.1913; found, 808.1910.

Compound 2 (Bzppy-OMe)₂Ir(acac). The yield of 65%. ¹H-NMR (300 MHz, CDCl₃): δ ppm 8.80 (d, *J* = 2.0 Hz, 2H), 8.25 (dd, *J* = 2.0, 8.6 Hz, 2H), 7.84 (d, *J* = 8.7, 2H), 7.79 (d, *J* = 7.7 Hz, 4H), 7.61 (d, *J* = 8.7 Hz, 4H), 7.53–7.48 (m, 4H), 6.46 (dd, *J* = 2.5 Hz, 8.6 Hz, 2H), 5.79 (d, *J* = 2.5 Hz, 2H), 5.28 (s, 1H), 3.56 (s, 6H), 1.55 (s, 6H). ¹³C-NMR (125 MHz, CDCl₃): δ ppm 192.9, 185.1, 171.9, 161.4, 152.8, 151.2, 138.5, 137.3, 136.6, 132.9, 130.0, 129.2, 128.9, 127.7, 118.4, 117.6,

107.6, 101.0, 54.9, 28.9. FT-IR (KBr): ν = 3058, 2936, 2834, 1656, 1581, 1543, 1516, 1398, 1314, 1275, 1214, 1176, 1039, 729 cm^{-1} . FAB-MS (m/z): 868 [M^+]. HRMS-FAB⁺ calcd for $\text{C}_{43}\text{H}_{35}\text{IrN}_2\text{O}_6$: 868.2125. found: 868.2139.

Compound 3 (*Bzppy-CF₃*)₂*Ir(acac)*. The yield of 50%. ¹H-NMR (300 MHz, CDCl_3): δ ppm 8.85 (d, J = 1.9 Hz, 2H), 8.36 (dd, J = 2.0, 8.4 Hz, 2H), 8.08 (d, J = 8.6 Hz, 2H), 7.82–7.79 (m, 4H), 7.74 (d, J = 8.1 Hz, 2H), 7.63–7.60 (m, 2H), 7.54–7.49 (m, 4H), 7.14 (d, J = 7.7 Hz, 2H), 6.50 (s, 2H), 5.23 (s, 1H), 1.53 (s, 6H). ¹³C-NMR (125 MHz, CDCl_3): δ ppm 192.4, 185.5, 170.7, 150.7, 149.4, 147.2, 139.4, 136.7, 133.4, 131.9, 131.3 (d, J = 31.0 Hz), 130.1, 129.4 (d, J = 3.7 Hz), 129.0, 125.5, 122.9, 119.4, 118.5 (d, J = 3.7 Hz), 101.2, 28.7. FT-IR (KBr): ν = 3064, 1663, 1600, 1564, 1516, 1397, 1379, 1315, 1284, 1265, 1163, 1122, 1073, 949, 910, 733, 714 cm^{-1} . FAB-MS (m/z): 944 [M^+]. HRMS-FAB⁺ calcd for $\text{C}_{43}\text{H}_{29}\text{F}_6\text{IrN}_2\text{O}_4$ 944.1661: found, 944.1659.

Synthesis of L2. A mixture of 5-benzoyl-2-bromopyridine (0.5 g, 1.91 mmol), 4-methoxyphenylboronic acid (0.32 g, 2.10 mmol), tetrakis(triphenylphosphine)palladium (0.09 g, 0.076 mmol), toluene (15 mL), ethanol (5 mL), and 2 M Na_2CO_3 (2.0 g, 19.1 mmol) was refluxed at 120°C for 5 h. After reaction mixture was cooled to room temperature, it was poured into water and extracted with ethyl acetate. The combined organic layer was dried with anhydrous MgSO_4 and evaporated to dryness. The crude product was further purified by silica gel column chromatography with 5:1 ethyl acetate:hexane as eluent. The product was a white solid with an isolated yield of 98% (0.54 g). ¹H-NMR (300 MHz, CDCl_3): δ ppm 9.04 (d, J = 2.2 Hz, 1H), 8.19 (dd, J = 2.2, 8.3 Hz, 1H), 8.07 (d, J = 8.9 Hz, 2H), 7.84 (t, J = 8.3 Hz, 3H), 7.67–7.62 (m, 1H), 7.55–7.50 (m, 2H), 7.04 (d, J = 8.9 Hz, 2H), 3.89 (s, 3H). ¹³C-NMR (125 MHz, CDCl_3): δ ppm 195.01, 161.61, 160.25, 151.59, 138.42, 137.43, 133.15, 131.00, 130.76, 130.20, 129.05, 128.81, 119.26, 114.59, 55.68. FT-IR (KBr): ν = 2959, 1642, 1586, 1450, 1251, 1043, 1022, 836, 798, 767, 704 cm^{-1} . EI-MS (m/z): 289 [M^+]. HRMS-EI⁺ calcd for $\text{C}_{19}\text{H}_{15}\text{O}_2\text{N}$ 289.1103: found, 289.1103.

Synthesis of L3. The reaction described for the synthesis of L1 was carried out starting with 5-benzoyl-2-bromopyridine (0.4 g, 1.53 mmol) and 4-(trifluoromethyl)phenylboronic acid (0.35 g, 1.83 mmol). After purification by chromatography on silica gel with 2:1 dichloromethane:hexane as eluent. The product was a white solid with an isolated yield of 96% (0.48 g). ¹H-NMR (300 MHz, CDCl_3): δ ppm 9.10 (dd, J = 0.8, 2.2 Hz, 1H), 8.26 (dd, J = 2.2, 8.3 Hz, 1H), 8.22 (d, J = 8.2 Hz, 2H), 7.93 (dd, J = 0.8, 8.3 Hz, 1H), 7.88–7.85 (m, 2H), 7.78 (d, J = 8.2 Hz, 2H), 7.67–7.64 (m, 1H), 7.57–7.52 (m, 2H). ¹³C-NMR (125 MHz, CDCl_3): δ ppm 194.7, 158.9, 151.5, 141.7 (d, J = 1.2 Hz), 138.7, 137.0, 133.5, 132.3, 131.9 (d, J = 32.8 Hz), 130.3, 128.9, 127.9, 126.1 (q, J = 3.7 Hz), 124.3 (d, J = 273. Hz), 120.5. FT-IR (KBr): ν = 1639, 1586, 1336, 1316, 1287, 1170, 1114, 1072, 1015, 841, 700 cm^{-1} . EI-MS (m/z): 327 [M^+]. HRMS-EI⁺ calcd for $\text{C}_{19}\text{H}_{12}\text{F}_3\text{NO}$ 327.0871: found, 327.0870.

Materials and Measurements

Phenylboronic acid, 2,5-Dibromopyridine, and *N,N*-Dimethylbenzamide were used as received from Aldrich or TCI. 5-Benzoyl-2-bromopyridine [16] were synthesized

as reported previously. The solvent were dried using standard procedures. All reagents were used as received from commercial sources, unless otherwise stated. All reactions were performed under N₂ atmosphere. ¹H- and ¹³C-NMR were obtained using a Varian (Unity Inova 300Nb) or Varian (Unity Inova 500NB) spectrometer at 300 MHz and 500 MHz, respectively. FT-IR spectra were recorded using a Thermo Nicolet Avatar 320 FT-IR spectrometer. Low- and high-resolution mass spectra were recorded using a Jeol JMS-AX505WA spectrometer in FAB mode or a Jeol JMS-600 spectrometer in EI mode.

Fabrication of OLEDs

The OLEDs using a red dopant in the emitting layers were fabricated by high vacuum (5.0×10^{-7} Torr) thermal deposition of organic materials onto the surface of an indium thin oxide (ITO, 30 Ω/sq, 80 nm)-coated glass substrate. The ITO glass was first cleaned with acetone, methanol, distilled water, and isopropyl alcohol. The organic materials were deposited in the following sequence: 65 nm of 4,4-bis[*N*-(1-(naphthyl)-*N*-phenyl-amino)biphenyl (NPB) was applied as a hole transporting layer (HTL), followed by a 30 nm thick emissive layer of the Ir^{III} complex doped in 4,4',*N,N'*-dicarbazolebiphenyl (CBP). The doping rate of the phosphor, an Ir^{III} complex, was 8%. Next, 10 nm thick bathocuproine (BCP), 25 nm thick tris-(8-hydroxyquinoline) aluminum (Alq₃), and 2 nm thick lithium quinolate (Liq) were deposited as a hole blocking layer, an electron transporting layer, and an electron injection layer, respectively. The typical organic deposition rate was 0.1 nm/s. Finally, 100 nm of Al was deposited as a cathode. The active areas of the OLEDs were 0.09 cm². After fabrication, the current-voltage (J-V) characteristics of the OLEDs were measured with a source measure unit (Keithley 236). The luminance and CIE chromaticity coordinates of the fabricated devices were measured using a chromameter (MINOLTA CS-100A). Electroluminescence was measured using LS-50B. All measurements were performed in ambient conditions under DC voltage bias.

Table 1. Optical properties of compounds

Compound	λ_{\max}^a [nm]	λ_{\max}^a [nm]	FWHM [nm]	HOMO/LUMO ^b [eV]	E _g	Φ ^c
(Bzppy) ₂ Ir(acac)	289 (0.431), 330 (0.430), 522 (0.020)	619	54	−5.56/−3.34	2.22	0.29
(Bzppy-OMe) ₂ Ir(acac)	280 (3.311), 345 (0.370), 494 (0.064)	599	82	−5.56/−3.23	2.37	0.55
(Bzppy-CF ₃) ₂ Ir(acac)	280 (3.374), 506 (0.045)	600	76	−5.93/−3.59	2.34	0.57

^aMaximum absorption or emission wavelength, measured in CH₂Cl₂ solution.

^bObtained from AC-2 and UV-vis absorption measurements.

^cUsing fac-[Ir(ppy)₃] as a standard; λ_{ex} = 400 nm (Φ_p = 0.40 in CH₂Cl₂).

Table 2. EL performance characteristic of the doped-devices

Device (compound)	V_{on}^a [V]	λ_{max}^{EL} [nm]	L^b [cd/m ²]	J^b [mA/ cm ²]	$LE^{c/d}$ [cd/A]	$PE^{c/d}$ [lm/W]	QE^d [%]	CIE^e (x,y)
1	7.0	606	5994	71	17.7/ 15.3	11.8/ 5.93	6.55	(0.610, 0.380)
2	6.0	571	34700	194	40.5/ 30.4	29.9/ 10.1	8.23	(0.486, 0.512)
3	6.3	593	15300	183	15.6/ 12.6	9.23/ 4.17	6.86	(0.570, 0.428)

^aTurn-on voltage at 1 cd/m².
^bMaximum luminance and current density.
^cMaximum value.
^dAt 20 mA/cm².
^eCommission Internationale d'Éclairage (CIE) coordinates at a 12.0 V.

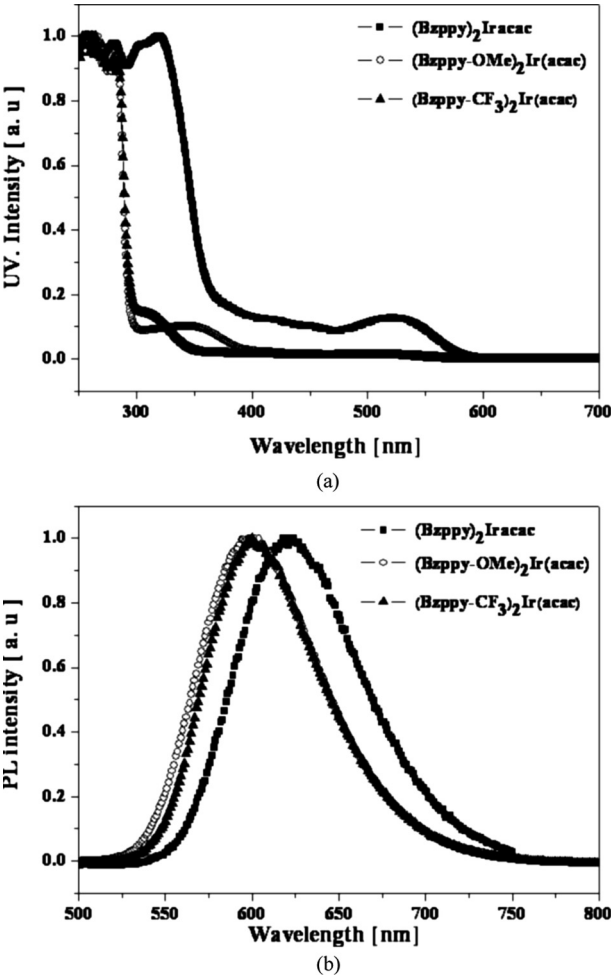


Figure 1. (a) The absorption and (b) emission spectra of compounds 1–3.

Results and Discussion

The optical properties of the red Ir(III) complexes ((Bzppy)₂Ir(acac), (Bzppy-OMe)₂Ir(acac), and (Bzppy-CF₃)₂Ir(acac)) were presented in Table 1. The HOMO energy levels were measured by a low-energy photo-electron spectrometer (Riken-Keiki AC-2). The HOMO/LUMO energy levels of (Bzppy)₂Ir(acac), (Bzppy-OMe)₂Ir(acac), and (Bzppy-CF₃)₂Ir(acac) were $-5.56/-3.34$, $-5.56/-3.23$, and $-5.93/-3.59$, respectively. In case of 3 with electro-withdrawing group, the HOMO/LUMO energy levels lower than those of 1.

The absorption and emission spectra of the Ir(III) complexes are shown in Figure 1. In the absorption spectra, the intense absorption bands located at 250 and 400 nm were assigned the spin-allowed $^1\pi-\pi^*$ transition of the cyclometalated ligands in the Ir(III) complexes and the weak and broad absorption bands at 400–470 nm assigned to spin-allowed metal-to-ligand charge transfer $^1\text{MLCT}$ transitions [17,18]. In addition, all complexes showed weaker absorptions longer than 470 nm, attributed to spin forbidden $^3\text{MLCT}/^3\pi-\pi^*$ transitions from the spin-orbit coupling of Ir(III), according to the band position and size [17]. This result revealed the strong $^3\text{MLCT}$ energy bands, with corresponding λ_{max} values of 520 nm for 1–3. The maximum emission wavelength (λ_{max}) of 1–3 appeared at 619, 599, and 600 nm, respectively. Compared to complex 1, complex 2 and 3 with methoxy (-OMe) group or trifluoromethyl (-CF₃) group in the phenyl unit was blue-shifted (ca. 19–20 nm) in the PL spectrum. Their emission quantum yield were 0.29, 0.55, and 0.57, respectively, as determined with Ir(ppy)₃ (0.40), used as a reference [19]. Interestingly, compounds 2 and 3, bearing, electro-donating (-OMe), and electro-withdrawing (-CF₃) groups in the phenyl unit, had quantum yields higher than that of Ir(ppy)₃.

The electroluminescent properties of complexes 1–3 were explored by employing the complexes as a dopant material in the fabrication of multilayered organic light-emitting diodes (OLEDs). As shown in Figure 3, devices 1–3 emitted in the red-orange region at 606, 571, and 593 nm, respectively. Compared to 1, both 2 with electro-donating and 3 with electro-withdrawing groups were blue shifted similarly

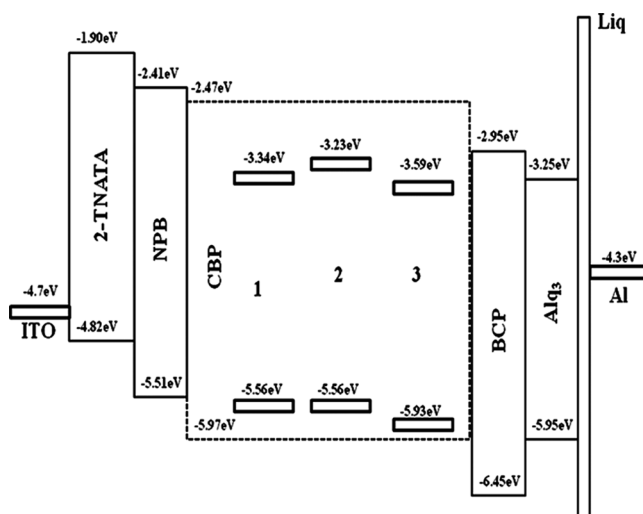


Figure 2. Energy-level diagram of OLEDs.

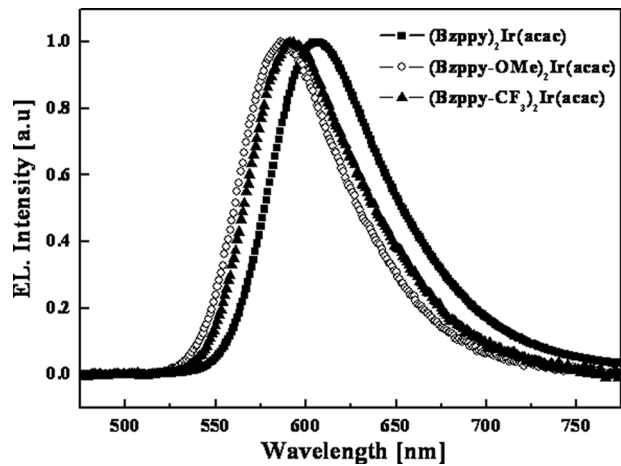


Figure 3. EL spectra of OLED devices 1–3.

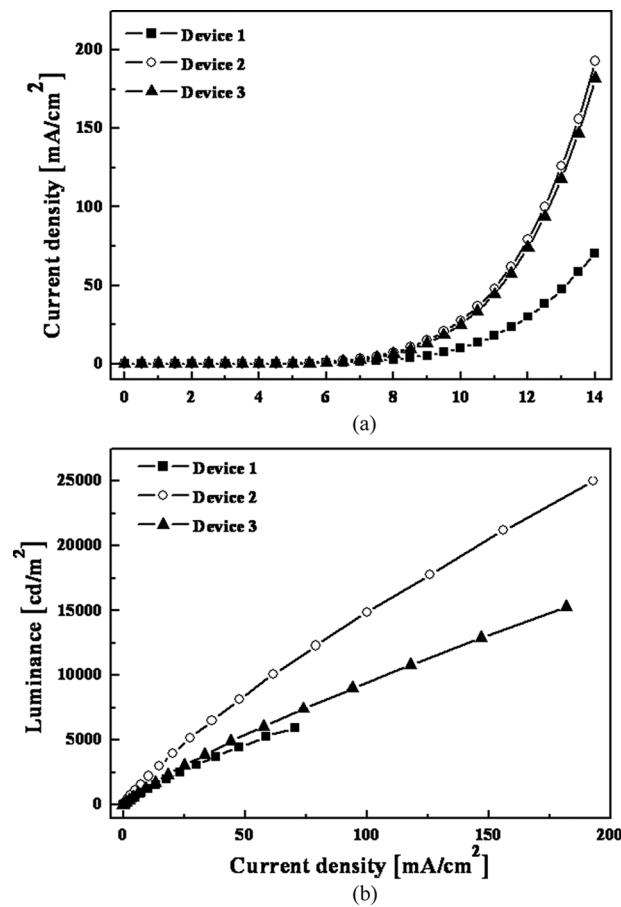


Figure 4. (a) Current density and (b) Luminance vs. voltage curves of OLED the devices 1–3.

in PL and EL spectra. However, complex 2 with electro-donating group in more blue shifted than with electro-withdrawing group complex 3 in EL spectra. The CIE coordinates of the devices were (0.610, 0.380), (0.486, 0.512), and (0.570, 0.428) at 12.0 V, respectively. The current density-voltage-luminance (J-V-L) characteristics are shown in Figure 4. The maximum luminances were 5994, 34700, and 15300 cd/m^2 at 14.0 V, respectively, with device 2 showing the highest luminance at this operating voltage. The luminous, and power efficiencies with respect to current density of the devices 1–3 were shown in Figure 5. The luminous efficiencies were 11.0, 30.4, and 12.6 cd/A at 20 mA/cm^2 , respectively. The devices 1–3 showed power efficiencies of 3.1, 10.1, and 4.17 lm/W at 20 mA/cm^2 , respectively. The EL performances were sensitive to the dopant structure within the emitting layer. In particular, an OLED device employing 2 as a dopant exhibited the best performance with a maximum

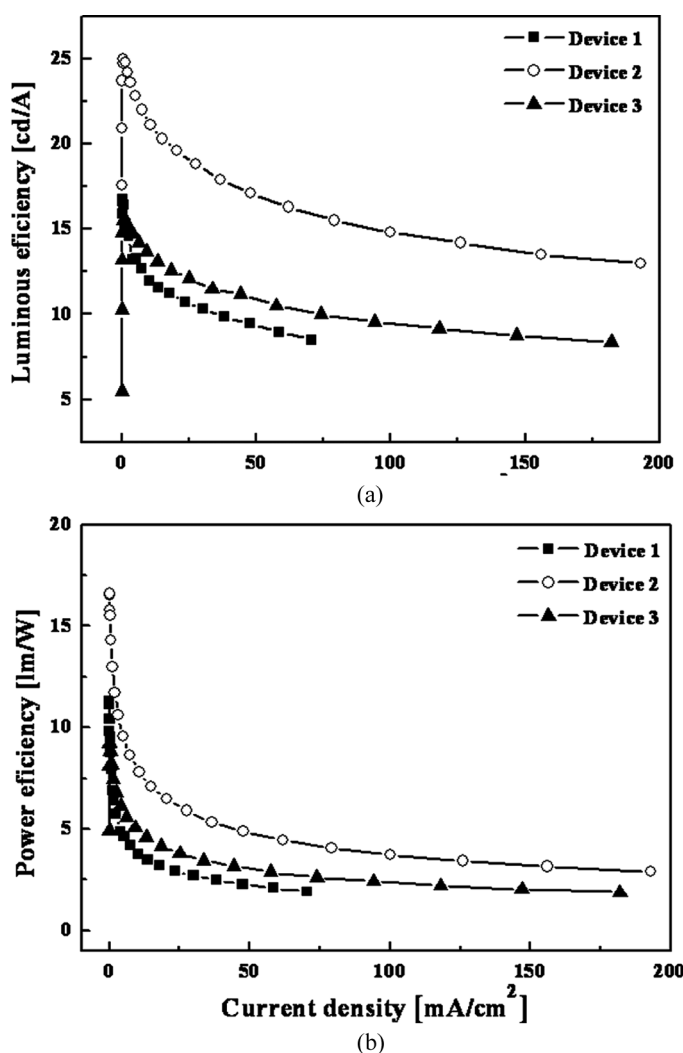
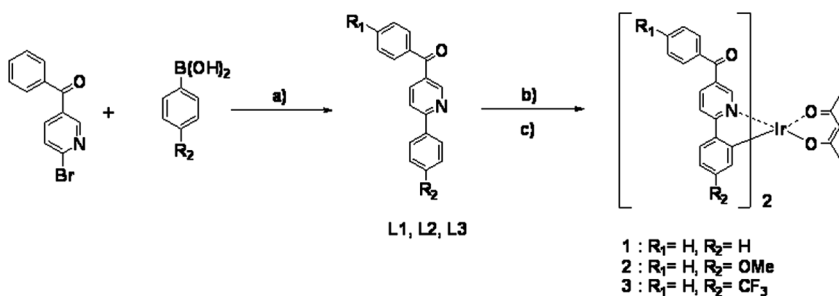


Figure 5. (a) Luminance, and (b) Power efficiency vs. current density curves of OLED device 1–3.



Scheme 1. Synthetic route to new iridium complexes 1–3. *Conditions:* a) $\text{Pd}(\text{PPh}_3)_4$, 2 M Na_2CO_3 , EtOH, toluene, 2 h, reflux. b) $\text{IrCl}_3 \cdot \text{H}_2\text{O}$, H_2O , 2-ethoxyethanol, 120°C , 24 h. c) 2,4-pentanedione, Na_2CO_3 , 2-ethoxyethanol, 100°C , 6 h.

luminance of 34700 cd/m^2 at 14.0 V and a luminous efficiency of 30.4 cd/A at 20 mA/cm^2 , respectively. In addition, this device showed orange emissions with CIE coordinates of (0.486, 0.512) at 12.0 V. This study demonstrates that phosphorescent Ir(III) complexes with benzoylated phenylpyridine possess excellent properties for red-orange emitting materials for OLEDs. Presumably, the electron-donating (-OMe) groups on the phosphorescent Ir(III) complexes could contribute to improved OLED efficiency by tuning the energy levels and charge transporting properties of the emitting materials in the solid state device. This highly efficient orange-red emitting iridium complexes could be used in the WOLED. Although white emission in OLED can be achieved by a mixture of the three primary colors (red, green, blue), highly efficient WOLEDs by fabrication devices composed of two emitters with complementary colors such as sky-blue and orange-red have been demonstrated [20,21]. Thereby, the highly efficient orange-red emitting material 2 can be combined with suitable sky-blue emitting materials to fabricate efficient WOLEDs.

Conclusion

We have synthesized the efficient red phosphorescent Ir(III) complexes with benzoylated phenylpyridine ligands. The OLED device employing 2 as a dopant exhibits the best performance with a maximum luminance of 34700 cd/m^2 at 14.0 V, and a luminous efficiency of 30.40 cd/A at 20 mA/cm^2 , respectively. The device showed orange-red emission with CIE coordinates of (0.486, 0.512) at 12.0 V. This study shows that the slightly structural difference of ligands affect the electroluminescent properties of the Ir(III) complexes in OLEDs.

References

- [1] Holder, E., Langeveld, B. M. W., & Schubert, U. S. (2005). *Adv. Mater.*, 17, 1109.
- [2] Chou, P.-T., & Chi, Y. (2007). *Chem. Eur. J.*, 13, 380.
- [3] Yersin, H. (2004). *Top. Curr. Chem.*, 241, 1.
- [4] Tokito, S., Iijima, T., Suzuri, Y., Kita, H., Tsuzuki, T., & Sato, F. (2003). *Appl. Phys. Lett.*, 83, 569.
- [5] Adachi, C., Baldo, M. A., Thompson, M. E., & Forrest, S. R. (2001). *J. Appl. Phys.*, 90, 5048.

- [6] Ikai, M., Tokito, S., Sakamoto, Y., Suzuki, T., & Taga, Y. (2001). *Appl. Phys. Lett.*, *79*, 156.
- [7] Thompson, M. E., Burrows, P. E., & Forest, S. R. (1999). *Curr. Opin. Solid State Mater. Sci.*, *4*, 369.
- [8] Wong, W., Zhou, G., Yu, X., Kwok, H., & Tang, B. (2006). *Adv. Funct. Mater.*, *16*, 838.
- [9] Thomas, K. R. J., Velusamy, M., Lin, J. T., Chien, C. H., Tao, Y. T., Wen, Y. S., Hu, Y. H., & Chou, P. T. (2005). *Inorg. Chem.*, *44*, 5677.
- [10] Lowry, M. S., & Bernhard, S. (2006). *Chem. Eur. J.*, *12*, 7970.
- [11] Lowry, M. S., Hudson, W. R., Pascal, R. A. Jr., & Bernhard, S. (2004). *J. Am. Chem. Soc.*, *126*, 14129.
- [12] Lowry, M. S., Goldsmith, J. I., Slinker, J. D., Rohl, R., Pascal, R. A. Jr., Malliaras, G. G., & Bernhard, S. (2005). *Chem. Mater.*, *17*, 5712.
- [13] Laskar, I. R., & Chen, T.-M. (2004). *Chem. Mater.*, *16*, 111.
- [14] Coppo, P., Plummer, E. A., & De Cola, L. (2004). *Chem. Commun.*, 1774.
- [15] Khalikl, M. M. A., & Elnagdi, M. H. (2002). *Synthetic Communications*, *32*, 159.
- [16] Ricardo, M. D., Codina, P., Jose, M., Jose, R. M., & Jorge, S. S. (1981). *Eur. Pat. Appl.*, 38.
- [17] Lamansky, S., Djurovich, P., Murphy, D., Abdel-Razzaq, F., Lee, H. E., Adachi, C., Burrows, P. E., Forrest, S. R., & Thompson, M. E. (2001). *J. Am. Chem. Soc.*, *123*, 4304.
- [18] Colombo, M. G., Brunold, T. C., Riedener, T., Güdel, H. U., Förtsch, M., & Bürgi, H. (1994). *Inorg. Chem.*, *33*, 540.
- [19] King, K. A., Spellane, P. J., & Watts, R.-J. (1985). *J. Am. Chem. Soc.*, *107*, 1431.
- [20] Sun, Y., Giebink, N. C., Kanno, H., Ma, B., Thompson, M. E., & Forrest, S. R. (2006). *Nature*, *440*, 908.
- [21] Yook, K. S., Jeon, S. O., Joo, C. W., & Lee, J. Y. (2008). *Appl. Phys. Lett.*, *93*, 073302.